Finite Difference Solution for Radiative–Conductive Heat Transfer of a Semitransparent Polycarbonate Layer

Babak Safavisohi,[1] Ehsan Sharbati,[1] Cyrus Aghanajafi,[2] Seyed Reza Khatami Firoozabadi[2]

[1]*Department of Mechanical Engineering, University of Saskatchewan, 57 Campus Drive, Saskatoon S7N 5A9, Canada*
[2]*Department of Mechanical Engineering, Khajeh Nasir University of Technology, Tehran, Iran*

Received 28 January 2008; accepted 4 July 2008
DOI 10.1002/app.29356
Published online 6 March 2009 in Wiley InterScience (www.interscience.wiley.com).

ABSTRACT: Thermal radiation greatly affects the transient thermal response of translucent materials in many practical applications, such as radiative heat shields and ignition and flame spreads for translucent plastics. However, because of the complexities that transients impose, less work has been done on the transient analysis of combined radiation–conduction heat transfer than on steady-state analysis. In this study, the transient heat transfer analysis of a polycarbonate (PC) layer was done with the use of the two-flux method and implicit finite difference formulations. The radiative and conductive properties of PC available in the literature, together with computer implementation prepared on the basis of the two-flux method and implicit finite difference formulations, were used to obtain the transient thermal response of a PC layer. On the basis of these results, we show that, compared to the conduction-alone case, the PC layer responded faster when radiation effects were considered. It is also shown that the internal reflectivity of boundaries had a great effect on the thermal response of the layer, whereas the thermal conductivity had a minor influence. © 2009 Wiley Periodicals, Inc. J Appl Polym Sci 112: 3313–3321, 2009

Key words: polycarbonates; radiation; thin films

INTRODUCTION

In translucent materials, energy can be transferred internally by radiation in addition to conduction. Because radiative heat flux propagates very rapidly, it can provide energy within a material more quickly than diffusion by heat conduction. As a result, transient temperature distribution including radiation can be much more different than that by conduction alone. For instance, when a translucent material is at high temperature, placed in a high-temperature surrounding, or subjected to large incident radiation, the radiative thermal effects become more dominant. Radiative effects in heat transfer have practical uses, including ignition and flame spread for translucent plastics, heat transfer analyses of porous ceramic insulation systems, removal of ice layers, formation and tempering of glass windows, evaluation of ceramic components, thermal protection coatings, and other scientific and engineering applications that involve the heating and formation of optical materials.

When a hot translucent layer is cooled by radiation to a lower temperature surrounding, energy is also lost within the body, and the interior can cool more rapidly than by conduction alone. On the other hand, if the radiative surroundings are hotter than the layer, the reverse effect can happen to the layer. In fact, depending on whether the radiative surroundings are hotter or cooler than the layer, this surrounding medium can act as a negative or positive internal heat source. Furthermore, a significant internal emission will also occur when the material is hot. This means that energy can be transmitted from one part of the layer to other parts by radiation in a larger quantity than by conduction alone. Thus, the transient (and steady-state) thermal response can be much different when both radiation and conduction are included. However, the quantity of energy transmitted by radiation depends on the transparency of the layer. The more radiation energy the layer absorbs and scatters, the less transparent the layer is.

A glance at the literature already available on transient heat transfer reveals the fact that the transient thermal response when both radiation and conduction are included has been studied much less than the steady-state thermal response. The reason lies in the complexities that appear in transient radiation heat transfer. Some of the studies on transient heat transfer by radiation were done by Siegel.[1–3] In those studies, various methods, including direct integration[1] and the two-flux method,[2,3] were used to calculate radiative effects. The two-flux method was also used in the study in ref. 4 to analyze transient heat transfer for combined radiation and conduction

Correspondence to: E. Sharbati (ehs965@mail.usask.ca).

when different boundary conditions and radiation parameters were used. In ref. 5, the authors discuss the transient thermal response of a glass layer considering both radiation and conduction. The direct integration method was used the study in ref. 6 to analyze the transient heat transfer of nongrey plastics to investigate the effects of various parameters, such as spectrum shape and the convective heat transfer coefficient. This method was also used in the study in ref. 7 to model the semitransparent layer of an advanced fiber polymer. The scattering effects in the transient thermal response of a polyamide 6T layer were studied in ref. 8. Other numerical methods for the computation of radiative effects in transient heat transfer are discrete ordinates,[9–12] Hottel's zonal method,[13–15] radiative diffusion,[16] differential approximation,[17] various expansion methods,[18] and the Monte Carlo method.[19]

The thermal behavior of polycarbonate (PC), which is widely used in aerospace applications, is of significant importance because thermal stresses, which are present in such applications, can play a role in design considerations. Also, because of the use of PC in some contemporary automobile windshields and the presence of high temperatures in the production process, it is important to understand the transient behavior of this polymer. In this study, we performed the transient heat transfer analysis of a semitransparent PC layer for combined radiation and conduction numerically by the application of the two-flux and implicit finite difference methods. The major focus of this article is the effect of the conductivity and reflectivity on the transient heat transfer of the PC layer. In addition, the quality and quantity of radiation effects on the transient and steady-state thermal responses of the PC layer are discussed. To this end, the results obtained by conduction alone are compared with combined conduction–radiation results. Also, results obtained with the use of various values of external radiative flux are compared.

COMBINED CONDUCTION–RADIATION EQUATIONS OF HEAT TRANSFER

Consider the semitransparent layer shown in Figure 1 as a heat-conducting, gray-emitting, absorbing, and isotropically scattering medium whose refractive index is greater than 1. This layer can exchange radiation energy with the radiative surroundings at both ends. Furthermore, the layer can be subjected to a constant temperature, a constant heat flux, and convection at either end. The general form of a one-dimensional heat transfer equation is

$$\rho c \frac{\partial T(x,t)}{\partial t} = \frac{\partial}{\partial x}\left(k(T)\frac{\partial T(x,t)}{\partial x}\right) + \dot{q}_{\text{gen}}(x,t) - \frac{\partial \dot{q}_r}{\partial x} \quad (1)$$

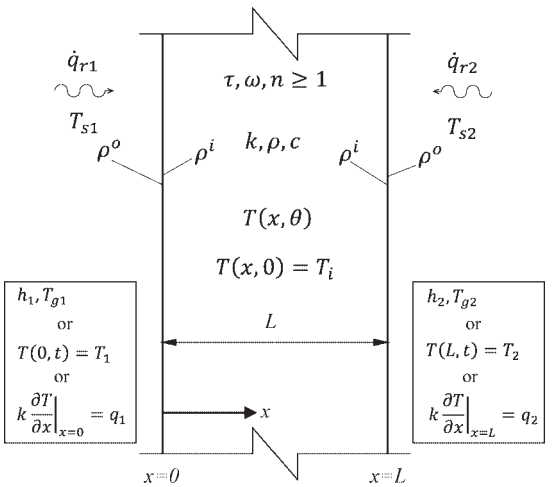

Figure 1 Geometry, material properties, and boundary conditions for the semitransparent layer whose transient thermal response was analyzed.

where ρ is the density, c is the specific heat, T is the absolute temperature, x is the coordinate in the direction across the layer, t is the time, k is the thermal conductivity, $\dot{q}_{\text{gen}}$ is the heat generation source (per unit volume), and $\dot{q}_r$ is the radiative heat flux. There are several methods for computing the gradient of radiative heat flux appearing in eq. (1). We computed this term, which represents radiation effects, with the use of the two-flux method. In accordance with the Mile–Eddington approximation, we have[20]

$$\frac{\partial \tilde{q}_r(X,t)}{\partial X} = \tau(1-\omega)\left[4n^2\Theta^4(X,t) - \tilde{G}(X,t)\right] \quad (2)$$

where $\tilde{q}_r$ is the dimensionless radiative heat flux, X is the dimensionless coordinate, τ is the optical thickness, ω is the scattering albedo, n is the refractive index, Θ is the dimensionless temperature (with respect to a reference temperature), and $\tilde{G}$ is a dimensionless radiative flux function, which is related to the radiative heat flux as follows:[3]

$$\frac{\partial \tilde{G}(X,t)}{\partial X} = -3\,\tau\,\tilde{q}_r(X,t) \quad (3)$$

By assuming the initial temperature of the layer (T_i) as the reference temperature, we could write the following expressions for the dimensionless parameters:

$$\tilde{q}_r = \dot{q}_r/\sigma T_i^4, \quad \Theta = T/T_i \quad (4)$$

where σ is the Stefan–Boltzmann constant. Equation (1) can also be written in a dimensionless form by the introduction of dimensionless time (θ), the dimensionless coordinate, and a radiation–conduction

parameter as follows in eq. (5) and substituting them into eq. (1) (see ref. 3):

$$\theta = 4\sigma T_i^3 t/\rho c L, \quad X = x/L, \quad N = k/4\sigma T_i^3 L \qquad (5)$$

where L is the thickness of the layer and N is the conduction–radiation parameter. However, because thermal conductivity (and even density and specific heat) can be a function of temperature, the dimensionless form of eq. (1) would not be appropriate for deriving a general finite difference formulation. Thus, differential eq. (1) and the corresponding boundary conditions are presented in a normal manner (with appropriate dimensions), whereas differential eqs. (2) and (3) and their corresponding boundary conditions are dimensionless.

Equations (1)–(3) are the governing differential equations of transient heat transfer for combined conduction–radiation in one dimension. A glance at these equations shows that obtaining the solution of these differential equations requires one initial condition and four boundary conditions. The initial condition can be simply the distribution of temperature at $t = 0$ throughout the layer. In this article, we assume that the layer is at an initial uniform temperature. This temperature is also used as the reference temperature [see eqs. (4) and (5)]. On the other hand, the four boundary conditions can be divided into two sets: the first set is the boundary conditions corresponding to conduction at either end of the layer, and the second set is the one concerning radiation at the two ends of the layer.

The simplest conduction boundary condition is constant temperature, which we can express by setting a given value for the temperature at any end of the layer. For the two other boundary condition types, which are convection and constant flux, we should note that energy is not absorbed at the boundary of the layer because the boundary itself has no volume for absorption. Consequently, in the absence of a spectral region in which the material is assumed opaque, the conduction boundary conditions are the same as with no radiation. Thus, the convection boundary condition is expressed in the following form:

$$k\frac{\partial T}{\partial x}\bigg|_{x=0} = -h_1\big(T_{g1} - T(0,t)\big) \qquad (6)$$

$$k\frac{\partial T}{\partial x}\bigg|_{x=L} = -h_2\big(T(L,t) - T_{g2}\big) \qquad (7)$$

where h_1 and h_2 are the convective heat transfer coefficients and T_{g1} and T_{g2} are the gas temperatures for convection at $x = 0$ and $x = L$, respectively. If any of the boundaries are subjected to a constant flux, the boundary condition can be written in the same form as eqs. (6) and (7) except that the right-hand side is replaced by the desired constant flux.

We can write the radiation boundary conditions at both ends of the layer by considering the incident and reflected fluxes in the following form:[21]

$$\tilde{G}(0,t) = 4\frac{1-\rho^o}{1-\rho^i}\tilde{q}_{r1} - 2\frac{1+\rho^i}{1-\rho^i}\tilde{q}_r(0,t) \qquad (8)$$

$$\tilde{G}(1,t) = 4\frac{1-\rho^o}{1-\rho^i}\tilde{q}_{r2} + 2\frac{1+\rho^i}{1-\rho^i}\tilde{q}_r(1,t) \qquad (9)$$

where ρ^i and ρ^o are the internal and external reflectivities, respectively, at the two boundaries of the layer and $\tilde{q}_{r1}$ and $\tilde{q}_{r2}$ are the dimensionless external radiation fluxes at $x = 0$ and $x = L$, respectively. If the temperature distribution is known throughout the layer, these two boundary conditions can be applied to obtain a unique solution for the differential eqs. (2) and (3). To be more precise, to obtain the solution of the transient heat transfer of a layer when radiation is included in addition to conduction, we need to solve differential eqs. (1)–(3) subjected to the boundary conditions mentioned in eqs. (6)–(9) and an initial condition, which in this article is a uniform temperature distribution at $t = 0$.

ANALYSIS METHODOLOGY AND NUMERICAL FORMULATION

Numerical analysis of the transient heat transfer of a layer in the absence of radiation can be done by the use of the conventional finite difference method. However, when radiation effects are included in heat transfer equations by the insertion of the gradient of radiative heat flux in the energy equation [eq. (1)], two more differential equations are added to the governing relations [eqs. (2) and (3)]. The term Θ,[4] appearing in eq. (2), makes these three equation coupled. Moreover, this term causes the governing differential equations to be nonlinear and the solution procedure to be extremely complex. To avoid the complexities appearing in nonlinear solution methods, we used a simple but effective method to solve these equations as follows: the solution procedure began with an initial condition, which was the temperature distribution throughout the layer. Because the temperature distribution was known, the differential eqs. (2) and (3) could be solved by the use of the boundary conditions presented in eqs. (8) and (9), and thus, the radiative flux function and dimensionless radiative heat flux could be computed. The gradient of radiative flux was then computed with eq. (2), and consequently, eq. (1) was solved with the usual finite difference method to obtain the temperature distribution at the next time step. The whole procedure was repeated by the use

of the temperature distribution that was just computed. This procedure did not include any nonlinear algorithm (e.g., the Newton–Raphson method), whereas the results based on it were proven to be accurate.[4] There were two main subprocedures in the computational process of each time increment, which were as follows:

1. The first subprocedure was the calculation of the gradient of radiative flux by the solution of the differential eqs. (2) and (3) with the boundary conditions in eqs. (8) and (9) and the temperature distribution of the previous time step. This was done with the common fourth-order Runge–Kutta method.[22] However, the boundary conditions required for the application of the common Runge–Kutta method should include values of the two unknown functions (which were the radiative flux function and dimensionless radiative heat flux here) for a given value of an independent variable (e.g., $x = 0$). Because the boundary conditions for the differential eqs. (2) and (3) included the values of unknown functions at $x = 0$ and $x = 1$, a shooting procedure, in addition to the common Runge–Kutta method, was also required to satisfy both boundary conditions at $x = 0$ and $x = 1$. An algorithm for the use of the shooting method is described in ref. 23. However, this method is usually time consuming because the numerical solution of the differential equation should be done several times to satisfy both boundary conditions. A representative method for the shooting procedure is to express each unknown function as a linear combination of two other unknown functions. The coefficient appearing in the combination is determined such that both boundary conditions are satisfied. A comprehensive discussion on this technique is explained in ref. 4. The advantage of this technique is that the numerical solution of the differential equation needs to be done only once; consequently, the solution procedure is less time consuming.
2. The second subprocedure was the use of the usual finite difference method together with the known values of the gradient of radiative heat flux, which was computed in the first subprocedure, to compute the temperature at the next time step. The implicit finite difference form of the energy equation for an interior grid point in the absence of heat generation source is[5]

$$\rho c \frac{T(x,t+\Delta t)-T(x,t)}{\Delta t} = (1-w)\frac{k(x)T(x-\Delta x,t)-(k(x+\Delta x)+k(x))T(x,t)+k(x+\Delta x)T(x+\Delta x,t)}{(\Delta x)^2} + w\frac{k(x)T(x-\Delta x,t+\Delta t)-(k(x+\Delta x)+k(x))T(x,t+\Delta t)+k(x+\Delta x)T(x+\Delta x,t+\Delta t)}{(\Delta x)^2} - \left.\frac{\partial \dot{q}_r}{\partial x}\right|_{x,t} \quad (10)$$

where Δt is the time increment, Δx is the distance between two successive grid points, and w is a weight coefficient for an implicit formulation representing the effect of the next time temperature. If the weight coefficient vanishes, the explicit form is obtained. Nonzero values for the weight coefficient results in implicit form. The thermal conductivity was assumed to be a function of x. This assumption enabled us to model materials with temperature-dependent thermal conductivity. On the other hand, the discrete form of the convection boundary conditions mentioned in eqs. (6) and (7) or any other form of boundary condition (e.g., constant flux and constant temperature) was written for the two grid points located in the boundaries of the layer. Writing eq. (10) for all interior grid points together with the two equations for the boundaries formed a tridiagonal linear system of equations in which the temperatures at the next time step were the unknowns.

The finite difference formulation, the two-flux method equations, and the methodology described in this section were used to prepare a computer implementation for the transient analysis of a layer for combined radiative–conductive heat transfer. The results presented in this article were obtained by the use of this computer implementation.

NUMERICAL RESULTS FOR A PC LAYER

In this section, the numerical results obtained on the bases of the computer implementation are presented. In the first step, the computer code was verified. To this end, some of the analyses done by Siegel in ref. 3 were repeated by the use of the computer implementation, and the results were compared. Figure 2 illustrates the temperature distribution during the transient of a layer subjected to convection at both ends when various values of scattering albedos were used. Other material properties are also presented in

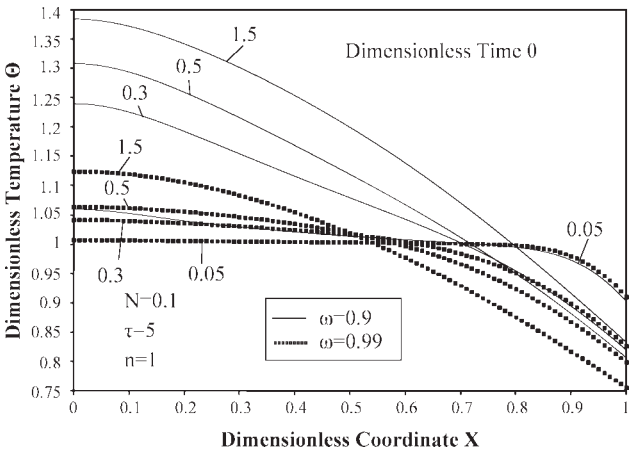

Figure 2 Temperature distribution in the transient interval for the layer subjected to convection at both ends with two values of scattering albedos. The parameters were $h_1 = 0$, $h_2 = 1$, $T_{g1} = 0.5T_i$, $\rho^i = 0$, $\rho^o = 0$, $\tilde{q}_{r1} = 1.5$,[4] and $\tilde{q}_{r2} = 0.5$.[4]

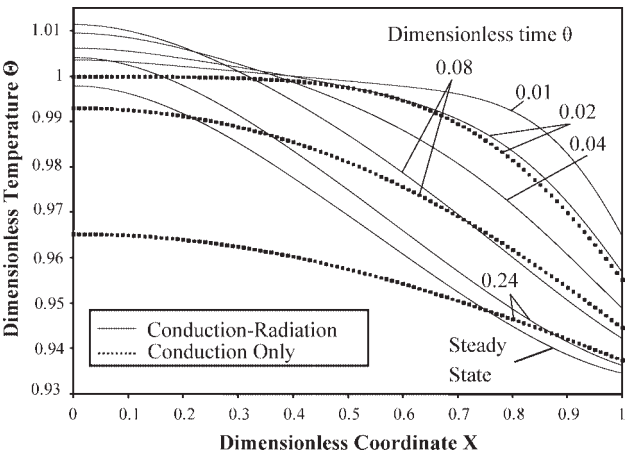

Figure 3 Transient thermal response of the PC layer insulated at $X = 0$ and cooled at $X = 1$ by convection. The parameters were $k = 0.19$, $h_1 = 0$, $h_2 = 40$, $T_{g2} = 0.93T_i$, $\rho^i = 0$, $\rho^o = 0$, $\tilde{q}_{r1} = 1.4$,[4] and $\tilde{q}_{r2} = 0.93$.[4]

the figure. The charts shown in Figure 1 coincide exactly with those presented in ref. 3. Several other analyses were also done, and the results were compared with the ones obtained by Siegel in ref. 3. These results are not presented here for brevity, but they all coincided with the results presented in ref. 3.

Consider a PC layer with a thickness of 0.3 cm that is at an initial temperature of 300 K and is subjected to radiative heat source at both ends. The thermal conductivity of the PC layer provided in handbooks includes a range of values instead of a single value. The main reason for variation in thermal conductivity is the variation of density and the speed of injection.[24] In accordance with the results obtained by Lasance in ref. 24, the thermal conductivity of PC lies in the range 0.19–0.22 W m^{-1} K^{-1}. Although the thermal conductivity affects the solution to differential eq. (1), the density and specific heat do not change the solution. In fact, the two parameters may only change the ratio of dimensionless time and the usual time expressed with dimensions [see eq. (6)]. To be more precise, presenting the results (including temperature distribution, radiative heat flux, and conductive heat flux) as functions of dimensionless time makes them more general. One may obtain results for a given material by using the corresponding values of density and specific heat.

Radiative parameters such as scattering and the absorption coefficient are discussed much less than conductive parameters such as the thermal conductivity. A procedure for calculating the scattering and absorption coefficients of different polymers were proposed by Wallner et al. in refs. 25 and 26. These results include the values of the scattering

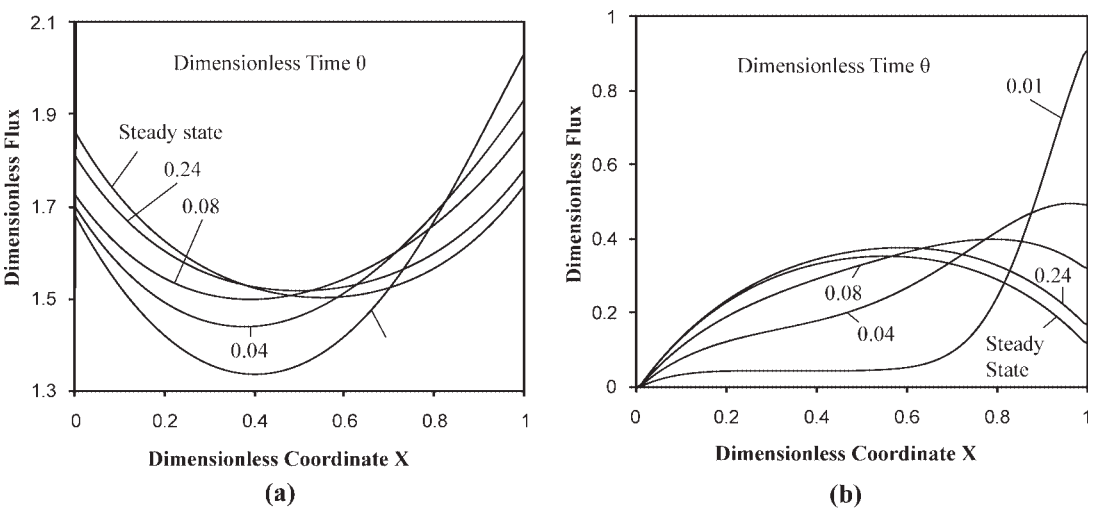

Figure 4 Radiative and conductive heat fluxes during the transient interval for the same analysis as shown in Figure 3: (a) radiative and (b) conductive heat fluxes.

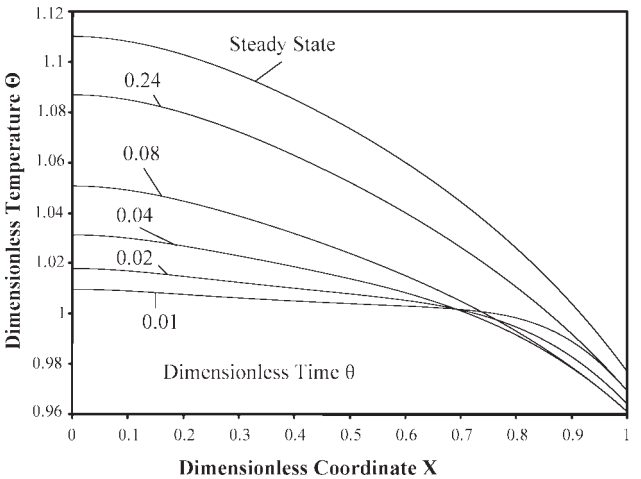

Figure 5 Transient thermal response of the PC layer insulated at $X = 0$ and cooled at $X = 1$ by convection. The parameters were $k = 0.19$, $h_1 = 0$, $h_2 = 40$, $T_{g2} = 0.93T_i$, $\rho^i = 0.5$, $\rho^o = 0$, $\tilde{q}_{r1} = 1.4$,[4] and $\tilde{q}_{r2} = 0.93$.[4]

coefficient[25] and absorption coefficients[26] as functions of the layer thickness. On the basis of these results, the values of optical thickness and scattering albedo for a PC layer with a thickness of 0.3 cm are approximately 1.08 and 0.0167, respectively. In addition, the value of the refractive index for a PC layer is 1.59.[25] With these material properties, the transient thermal response of the PC layer subjected to various conductive and radiative boundary conditions was examined, and the results are fully discussed.

Figure 3 illustrates the temperature distribution in the transient interval for the PC layer when the thermal conductivity was assumed to be 0.19 W m^{-1} K^{-1}. The layer was heated by radiation at $x = 0$ and cooled by convection at $x = L$. When $\theta = 0.8$ the temperatures were within 1% of steady state, which showed a relatively short transient interval. In addition, the temperature at $x = L$ decreased in the transient interval, whereas at $x = 0$, the temperature increased rapidly until $\theta = 4$ and then continued to decrease for the rest of the transient interval. However, in accordance with the steady-state temperature distribution, the overall result of the radiative and convective boundary conditions was the cooling of the whole layer. Figure 3 also includes the results obtained by conduction alone. In accordance with Figure 3, the temperature distribution was smoother when only conduction was considered. In this case, the temperature changed rapidly at the beginning of the transient interval; However, the steady-state temperature distribution, which was $T = 0.93T_i$, was reached at a very slow rate: the temperature at $x = 0$ and $\theta = 2$ was still 0.932.

The radiative and conductive heat fluxes for this analysis (for the conduction–radiation case) are shown in Figure 4(a,b). A comparison between the two figures shows that the radiative heat transfer was much greater than the conductive heat transfer throughout the transient interval. Although the temperature at $x = 0$ decreased because $\theta = 0.08$, the radiative heat flux increased during the whole transient interval.

So far in this study, the reflectivity was assumed to be zero at the two ends of the layer. The transient thermal response of the PC layer with the same material properties and boundary conditions as those in Figure 3 but with a value of 0.5 for ρ^i is presented in Figure 5. A comparison of Figures 3 and 5 shows that the thermal response of the layer totally changed when ρ^i was nonzero: the temperature at $x = 0$ increased throughout the transient interval, whereas at $x = L$, it decreased at first but continued to increase for the rest of the transient interval. In addition, the steady-state temperature distribution

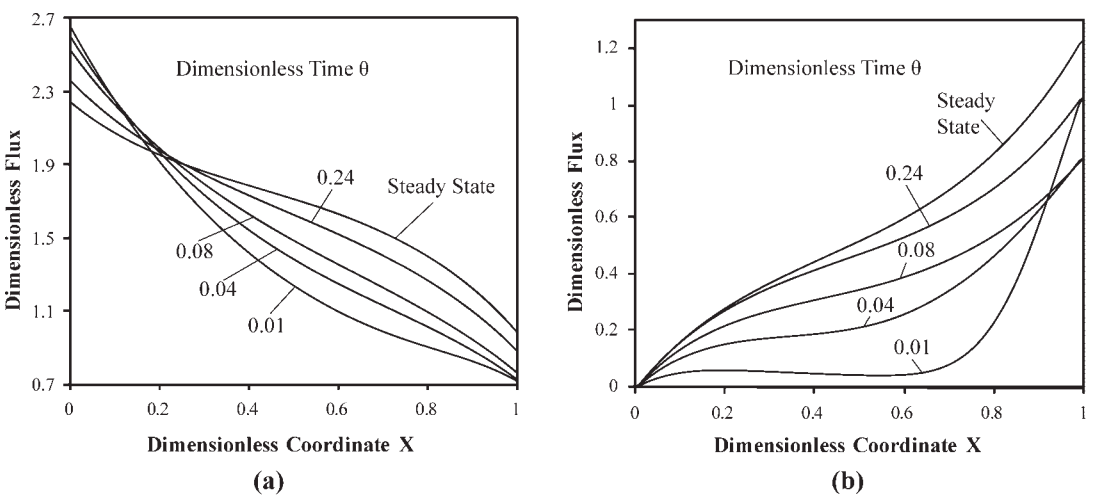

Figure 6 Radiative and conductive heat fluxes in the transient interval for the same analysis as shown in Figure 5: (a) radiative and (b) conductive heat fluxes.

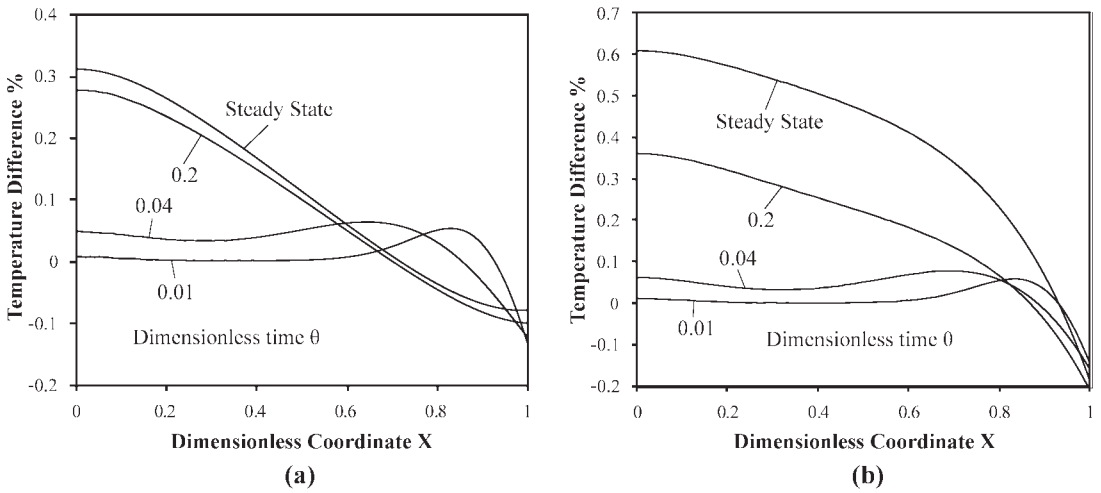

Figure 7 Difference between the temperatures obtained by $k = 0.19$ and $k = 0.21$ over the dimensionless coordinate for various values of dimensionless time. ρ^i = (a) 0 and (b) 0.5.

was above the initial temperature distribution except in the small part of the layer between $X = 0.93$ and $X = 1$. Consequently, the layer was heated (in most part) for $\rho^i = 0.5$, whereas it was cooled for $\rho^i = 0$. This may have been the direct effect of internal reflectivity, which did not let the radiation energy leave the layer and kept the layer warmer. Another effect of internal reflectivity was that the temperature variation during the transient interval and the temperature gradient through the layer were greater when ρ^i was 0.5.

Figure 6 presents the radiative and conductive heat fluxes during the transient interval for the analysis whose transient temperature distribution is shown in Figure 5. Although the temperature increased at $x = 0$ during the transient interval, the radiative heat flux decreased at this point. On the other hand, the radiative heat flux increased at $x = L$ in the transient interval, whereas the temperature did not show unique behavior at this point. A comparison between Figures 6(a) and 4(a) shows that the variation of radiative heat flux across the layer was greater for $\rho^i = 0.5$.

As mentioned earlier, the thermal conductivity of PC varied from 0.19 to 0.21 W m^{-1} K^{-1}. The two previous analyses were done with the lower value for the thermal conductivity. To present a more comprehensive study of the transient thermal response of a PC layer, these analyses were repeated this time with the assumption that the thermal conductivity was 0.21 W m^{-1} K^{-1}. Figure 7 illustrates the difference between the temperatures obtained by $k = 0.19$ and $k = 0.21$ throughout the layer for various values of dimensionless time. The dimensionless temperatures were used to compute the temperature difference in this figure. In accordance with the figure, the

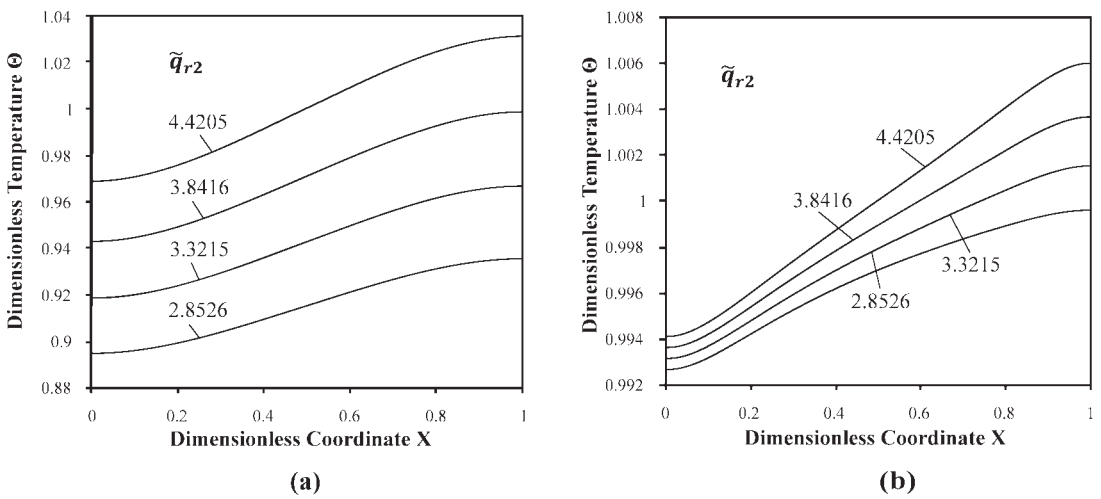

Figure 8 Temperature distribution for various values of the dimensionless external radiation flux at $x = L$. The other parameters were $k = 0.19$, $h_1 = 0$, $h_2 = 0$, $\rho^i = 0$, $\rho^o = 0$, and $\tilde{q}_{r1} = 0.9$.[4] (a) Steady state and (b) $\theta = 0.01$.

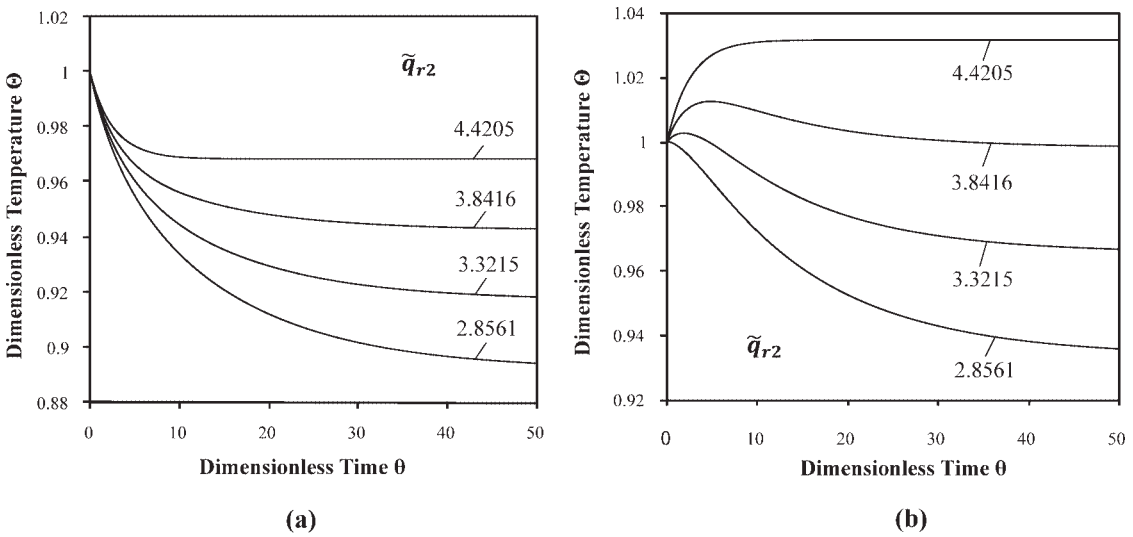

Figure 9 Temperature variation over time at the two ends of the layer. The parameters were the same as those listed for Figure 8. $X =$ (a) 0 and (b) 1.

maximum absolute difference occurring was 0.6% or 1.8 K. Thus, the results obtained with the two extreme values of thermal conductivity were approximately the same. In addition, the patterns of the curves in Figure 7(a,b) are similar for smaller values of dimensionless time.

To investigate the effects of the external radiative fluxes on the transient of a PC layer, a series of analyses were done with the convection boundary condition at both ends with a zero convective heat transfer coefficient. Consequently, the layer did not exchange conductive heat at the boundaries, and the external sources of energy were only produced by external radiative heat fluxes at the two ends. The radiative heat flux at $X = 0$ was the same in all of these analyses, whereas various values were used at $X = 1$. Figure 8 illustrates the temperature distribution for $\theta = 0.01$ and the steady state with various values of the dimensionless external radiation flux at $x = L$. The steady-state temperature profiles were approximately parallel with a constant distance between the curves. Also, the steady-state temperatures were less than the initial temperature for $\tilde{q}_{r2} =$ 2.8561, 3.3215, and 3.8416, which means that the whole layer was cooled despite the relatively large values of the dimensionless external radiation flux at $x = L$.

Figure 9 shows the variation of temperature over time for the same analyses. In the transient interval, the temperature decreased at $X = 0$ for all four values of the dimensionless external radiation flux at $x = L$. On the other hand, the temperature increased at $X = 1$ for larger values of the dimensionless external radiation flux at $x = L$. In addition, a glance at Figure 9(a,b) shows that the steady state was reached much faster for $\tilde{q}_{r2} = 4.4205$. More generally, the transient interval was longer when the dimensionless external radiation flux at $x = L$ decreased. This was what we expected because increasing the value of the dimensionless external radiation flux at $x = L$ made the effects of radiation more dominant, and consequently, the thermal response was faster.

CONCLUSIONS

The transient heat transfer analysis of a PC layer was done with the two-flux method and implicit finite difference formulations. The conductive boundary condition used in these analyses was convection, whereas various values of external radiative heat fluxes were used for the radiative boundary conditions. In addition, because the thermal conductivity of PC available in the literature included a range of values, the two extreme values of the thermal conductivity were used in the analyses.

As expected, the transient thermal responses of the PC layer obtained by consideration of the radiation effects were different from those obtained by conduction alone. The thermal response of the PC layer was relatively fast and the response was faster than in the conduction-alone case because the internal radiative heat flux was greater than the internal conductive heat flux. In general, this faster transient response could be used in applications where the material is required to heat (or cool) quickly. On the other hand, the temperature gradient was higher in the conduction–radiation case than in the conduction-alone case for some boundary conditions (see Fig. 3), whereas the reverse was true for other boundary conditions.[3] In conclusion, whether the inclusion of radiation effects led to a higher

temperature gradient (and, thus, higher thermal stresses) or a lower gradient depended on the boundary conditions.

The effect of the internal reflectivity of the boundaries was shown to be magnificent. The layer thermal response for $\rho^i = 0$ totally differed from that for $\rho^i = 0.5$: the temperature generally increased for $\rho^i = 0.5$, whereas it decreased for $\rho^i = 0$. Also, temperature changed more in the transient interval and throughout the layer for $\rho^i = 0.5$.

The temperature distributions obtained by the use of the two extreme values of thermal conductivity were proven to have little difference. On the other hand, various values of the external radiative heat flux at one end, when the external radiative heat flux at the other end was kept unchanged, resulted in different temperature distributions: the temperature increased when the external radiative heat flux increased such that the temperature profiles of the steady state were approximately parallel. Furthermore, the transient interval was shorter for larger values of external radiative heat flux.

NOMENCLATURE

c	Specific heat (J kg^{-1} K^{-1})
$\tilde{G}$	Dimensionless radiative flux function
h_1, h_2	Convective heat transfer coefficients (W m^{-2} K^{-1})
k	Thermal conductivity (W m^{-1} K^{-1})
L	Thickness of the layer (m)
n	Refractive index
N	Conduction–radiation parameter ($k/4\sigma T_i^3 L$)
$\dot{q}_{gen}$	Heat generation source (per unit volume)
$\dot{q}_r$	Radiative heat flux
$\tilde{q}_r$	Dimensionless radiative heat flux ($\dot{q}_r/\sigma T_i^4$)
$\dot{q}_{r1}$, $\dot{q}_{r2}$	External radiation fluxes at $x = 0$ and $x = L$, respectively
$\tilde{q}_{r1}$, $\tilde{q}_{r2}$	Dimensionless external radiation fluxes at $x = 0$ and $x = L$, respectively
t	Time (s)
T	Absolute temperature (K)
T_{g1}, T_{g2}	Gas temperatures for convection at $x = 0$ and $x = L$, respectively (K)
T_i	Initial temperature of the layer (K)
T_{s1}, T_{s2}	Gas temperatures for radiation at $x = 0$ and $x = L$, respectively (K)
w	Weight coefficient for implicit formulation representing the effect of next time temperature
x	Coordinate in the direction across the layer (m)
X	Dimensionless coordinate (x/L)
Δt	Time increment
Δx	Distance between two successive grid points
ω	Scattering albedo
ρ	Density (kg/m^3)
ρ^i, ρ^o	Internal and external reflectivities, respectively
σ	Stefan–Boltzmann constant (W m^{-2} K^{-4})
τ	Optical thickness
Θ	Dimensionless temperature (T/T_i)
θ	Dimensionless time ($4\sigma T_i^3 t/\rho c L$)

References

1. Siegel, R. Int J Heat Mass Transfer 1996, 39, 6.
2. Siegel, R. J Thermophys Heat Transfer 1996, 10, 681.
3. Siegel, R. Int J Heat Mass Transfer 1996, 39, 1111.
4. Sharbati, E.; Safavisohi, B.; Aghanajafi, C. J Fusion Energy 2004, 23, 207.
5. Safavisohi, B.; Sharbati, E.; Aghanajafi, C. In Proceedings of the Fourth International Conference on Computational Heat and Mass Transfer; Lavoisier Publications: Paris, France, 2005; pp 1041.
6. Sadooghi, P. J Vinyl Additive Technol 2005, 11, 28.
7. Sadooghi, P.; Aghanajafi, C. J Appl Polym Sci 2006, 100, 4181.
8. Sadooghi, P.; Aghanajafi, C. J Reinforced Plast Compos 2005, 24, 1655.
9. Su, M. H.; Sutton, W. H. 1995, 9, 370.
10. Gorthala, R.; Harris, K. T.; Roux, J. A.; McCarty, T. A. J Thermophys Heat Transfer 1994, 8, 125.
11. Sadooghi, P.; Aghanajafi, C. J Fusion Energy 2003, 22, 59.
12. Aghanajafi, C.; Dehghani, A. WSEAS Trans Heat Mass Transfer 2006, 1, 68.
13. Safavisohi, B.; Sharbati, E.; Aghanajafi, C.; Khatami, F. S. R. J Fusion Energy 2006, 25, 145.
14. Safavisohi, B.; Sharbati, E.; Aghanajafi, C.; Khatami, F. S. R. Proceedings of the 8th Biennial ASME Conference on Engineering Systems Design and Analysis; ASME Publication: Turin, Italy, 2006.
15. Sadooghi, P.; Aghanajafi, C. Radiat Effects Defects Solids 2004, 159, 61.
16. Petrov, V. A. Int J Heat Mass Transfer 1997, 40, 2241.
17. Wu, C. Y.; Ou, N. R. Int J Heat Mass Transfer 1994, 37, 2657.
18. Frankel, J. I. J Thermophys Heat Transfer 1995, 9, 210.
19. Derevyanko, G. V.; Koltun, P. S. J Eng Phys 1991, 61, 680.
20. Siegel, R.; Howell, J. R. Thermal Radiation Heat Transfer, 3rd ed.; Hemisphere: Washington, DC, 1992.
21. Siegel, R.; Spuckler, C. M. Int J Heat Mass Transfer 1994, 37, 403.
22. Kreyszig, E. Advanced Engineering Mathematics, 8th ed.; Wiley: New York, 1998.
23. Press, W. H.; Flannery, B. P.; Teukolsky, S. A.; Vetterling, W. T. Numerical Recipes FORTRAN Version; Cambridge University Press: Cambridge, 1989.
24. http://www.electronics-cooling.com/html/2001_may_techdata.html (access January 2006).
25. Wallner, G. M.; Platzer, W.; Lang, R. W. Solar Energy 2005, 79, 583.
26. Wallner, G. M.; Platzer, W.; Lang, R. W. Solar Energy 2005, 79, 593.